Video Article

Microscale Vortex-assisted Electroporator for Sequential Molecular Delivery

Dwayne A. L. Vickers[1], Soojung Claire Hur[1]

[1]The Rowland Institute, Harvard University

Correspondence to: Soojung Claire Hur at hur@rowland.harvard.edu

URL: http://www.jove.com/video/51702
DOI: doi:10.3791/51702

Keywords: Bioengineering, Issue 90, electroporation, microfluidics, cell isolation, inertial focusing, macromolecule delivery, molecular delivery mechanism

Date Published: 8/7/2014

Citation: Vickers, D.A.L., Hur, S.C. Microscale Vortex-assisted Electroporator for Sequential Molecular Delivery. *J. Vis. Exp.* (90), e51702, doi:10.3791/51702 (2014).

Abstract

Electroporation has received increasing attention in the past years, because it is a very powerful technique for physically introducing non-permeant exogenous molecular probes into cells. This work reports a microfluidic electroporation platform capable of performing multiple molecule delivery to mammalian cells with precise and molecular-dependent parameter control. The system's ability to isolate cells with uniform size distribution allows for less variation in electroporation efficiency per given electric field strength; hence enhanced sample viability. Moreover, its process visualization feature allows for observation of the fluorescent molecular uptake process in real-time, which permits prompt molecular delivery parameter adjustments *in situ* for efficiency enhancement. To show the vast capabilities of the reported platform, macromolecules with different sizes and electrical charges (*e.g.,* Dextran with MW of 3,000 and 70,000 Da) were delivered to metastatic breast cancer cells with high delivery efficiencies (>70%) for all tested molecules. The developed platform has proven its potential for use in the expansion of research fields where on-chip electroporation techniques can be beneficial.

Video Link

The video component of this article can be found at http://www.jove.com/video/51702/

Introduction

In recent years, the use of electric pulses to facilitate cytosolic delivery of extracellular molecules has become an attractive means of manipulating mammalian cells.[1] This process, also known as electroporation, reversibly permeabilizes the cellular membrane, allowing for inherently membrane impermeable molecules to gain access to the cells' intracellular milieu. Because virtually any molecule can be introduced into the cytosol via temporary created pores in the membrane of any type of cells using electroporation, the technique has been reported as being more reproducible, universally applicable, and more efficient than other methods including virus-mediated, chemical and optical approaches.[2-3] This technique has been utilized to introduce fluorescent molecules,[4] drugs[5] and nucleic acids[6-7] while keeping cells viable and intact. Given these benefits, electroporation has been adopted as a common laboratory technique for DNA transfection, *in vivo* gene therapy[8] and cell vaccination studies. It is, however, still difficult for conventional electroporation systems to simultaneously achieve practical efficiency and viability for samples with large heterogeneity in size because the electric field strength required for successful electroporation closely correlates with the cell's diameter. Moreover, those systems do not allow precise control of the multiple molecular amounts being delivered due to reliance on bulk stochastic molecular delivery process.[9] In order to address these issues, many groups have developed microfluidic electroporation platforms, offering the advantage of lower poration voltages, better transfection efficiency, a large reduction in cell mortality, and ability to deliver multiple molecules.[10-13] These advantages were made possible owing to the small footprints of microscale electroporation systems whose electrode pitch lengths are sub-millimeters, dramatically decreasing voltages required for successful delivery. Moreover, these microscale electroporation systems can achieve uniform electric field distribution and rapidly dissipate generated heat, yielding reduced cell mortality while enhancing delivery efficiency. The utilization of transparent materials for these microchips further allows *in situ* observation of the electroporation process for prompt parameter modifications.[2,12] However, precise dosage control and molecular- and cellular-dependent parameter control, required for emerging research and therapeutic applications,[6,14-16] still remain unresolved.

This work presents a microfluidic vortex-assisted electroporation system, capable of delivering multiple molecules sequentially into a pre-selected identical population of target cells. Cells with uniform size distribution are isolated prior to electroporation using previously reported size-selective trapping mechanism.[17-18] By having a uniform size distribution, less variation in electroporation efficiency and enhanced viability per given electric field strength were achieved.[19] Furthermore, continuously agitating trapped cells using microscale vortices allowed for uniform delivery of molecules across the entire cytosol, in agreement with the results previously reported using another vortex-assisted electroporation platform.[20] To demonstrate that this system would be applicable to a broad range of molecules commonly utilized in biological applications, macromolecules with a wide range of molecular weights were delivered to metastatic breast cancer cells. In addition, with the aid of real-time process monitoring, this work provides more evidence to put an end to the long standing debate regarding the mechanism of molecular delivery during electrporation, being predominantly electrophoresis-mediated versus diffusion-mediated.[14] Unlike other electroporation systems, this platform uniquely provides the combined advantages of precise multi-molecule delivery, high molecular delivery efficiency, minimal cell mortality, a wide span of size and charges of delivered molecules, as well as real-time visualization of the electroporation process. Given these

capabilities, the developed electroporation system has practical potential as a versatile tool for cellular reprogramming studies,[6,14,21-22] drug delivery applications[10,19] and applications requiring for in-depth understanding of electroporation molecular delivery mechanisms.

Protocol

1. Cell Preparation

1. Plate 1×10^5 cells/ml of metastatic breast cancer cell line MDA-MB-231 in a volume of 10 ml per tissue culture T75 flask in Leibovitz's L-15 Medium supplemented with 10% (v/v) fetal bovine serum and 1% penicillin-streptomycin.
2. Incubate MDA-MB-231 cells in a humidified incubator at 37 °C with 0% CO_2 environment.
3. Harvest cells for experiments 2 days after seeding by treating cells with 0.25% trypsin-EDTA for 2 min and inactivate trypsin's enzymatic activity by adding 8 ml of the growth media.
4. Pellet cells by centrifuging for 5 min at 200 × g and resuspend in Dulbecco's phosphate buffered saline (DPBS, 1x, without Ca^{2+} and Mg^{2+}) to a final concentration of 5×10^5 cells/ml.

2. Device Design and Fabrication

NOTE: The mask, master mold fabrications and the microchannel enclosing process are to be conducted inside a clean room while the polydimethylsiloxane (PDMS) microchannel casting process can be performed on a regular laboratory benchtop.

1. Design a microfluidic device as illustrated in **Figure 1** with AutoCAD. The device should consist of an inlet with multiple injection ports, coarse filters and two parallel straight rectangular inertial focusing channels (L = 7 mm, W = 40 μm, and H = 70 μm). Individual straight channel consists of 5 electroporation chambers, which are placed 800 μm apart (W_C = 400 μm) with two via holes for aluminum electrodes. Two transversally adjacent electroporation chambers share the hole for the negative electrode. Two straight channels merge into an outlet at the downstream of the electroporation region.
2. Convert the CAD file with micro-patterns to a GDSII file using LinkCAD. Write the micro-patterns on a 5" x 5" photomask blank using a laser mask writer. Develop the mask by following the manufacturer's protocol. NOTE: The mask development process includes photoresist developing, chrome etching and resist removal. Alternatively, micro-patterns printed on a high resolution transparency (>20,000 dpi) can be purchased from a third party manufacturer and used as a photomask. Final microscale features on a photomask should be transparent to match the polarity of a negative photoresist.
3. Fabricate the casting mold of the device design using standard soft lithography techniques[23] with a negative photoresist spun coat on a 4 inch silicon wafer at 2,000 rpm to have the final thickness of 70 μm.
4. Prebake the wafer with negative photoresist for 20 min at 95 °C.
5. Contact the mask with the wafer and expose to a UV source (17.4 mJ/cm^2) for 80 sec using a mask aligner.
6. Develop the exposed wafer for 4 min in a SU-8 developer.
7. Measure the developed photoresist thickness using a surface profilometer.
8. Rigorously mix a 10:1 ratio of elastomer to curing agent (silicone elastomer kit) and pour the mixture on the casting mold to generate PDMS replicas. Degas the casting elastomer for 30 min and cure the casting mold with degassed elastomer in an oven at 70 °C for 2 hr.
9. Delaminate cured PDMS replica with microchannel patterns from the mold and punch holes for inlets, outlet and electrode insertions using a pin vise. NOTE: The normal cutting edge diameter of the pin vise should be 0.76 mm, adequate for tightly holding PEEK tubing (O.D. of 1/32") and aluminum electrodes (O.D. of 0.029") in place.
10. Create enclosed microfluidic channels by bonding PDMS replicas to a glass slide treated in an oxygen-plasma cleaner for 7 sec at a radio frequency power and oxygen partial pressure of 75 W and 500 mTorr, respectively.

3. Flow Experiments

1. Insert aluminum electrodes (0.029" OD) and an outlet PEEK tubing (1/32" OD) into designated places via holes in the microchannel (see **Figure 3B**).
2. Connect the electrical equipment[18] responsible for generating high-voltage short square-wave pulses to the aluminum electrodes (see **Figure 3C**) that are in contact with flowing solutions in the PDMS mold. NOTE: The equipment should consist of a pulse generator and an in-house built high voltage amplifier.[18]
3. Prepare four 50 ml centrifuge tubes individually containing DPBS, solutions with cells and biomolecules, and attach each tube to its respective vial holder connected to the pneumatic flow control system (see **Figure 3A**).[18]
4. Connect inlet PEEK tubing from the vial holders into the respective inlet holes in the microfluidic device.
5. Set the magnitude of square-wave pulses, V, to 100 V in order to have the electric field strength, $E = V/L_e$, across the electroporation chamber be equivalent to 0.7 kV/cm. NOTE: Here, L_e is the distance between two points where the positive and negative electrodes are in contact with the flowing solution (see **Figure 1**).
6. Set the pressure regulator to 40 psi. NOTE: A single manually adjustable nitrogen source is used to uniformly pressurize all sample vials and a high-speed manifold is utilized to timely activate individual solution ports using the custom-built LabVIEW software.[18]
7. For valve control, open the custom-built LabVIEW software labeled *Valve Runner*, and click run from the dropdown menu entitled operate.
8. Turn on valves by clicking on each corresponding valve icon. NOTE: The valve icon should turn green when it is activated. Clicking the active icon will deactivate and close the valve. The closed valve icon should turn grey.
9. Open the valve for the DPBS reservoir (*i.e.*, washing solution) to prime the flow speed required for stable cell-trapping vortex generation for 1.5 min.
10. Switch the active solution port from the washing solution to the cell solution to trap cells in the electroporation chamber for 30 sec (*i.e.*, the cell-trapping step).

11. Flow both washing and cell solutions through the device simultaneously for 10 sec prior to the cell-trapping step to ensure undisrupted flow during the solution-switching step. NOTE: This brief co-flow step should be repeated at each solution-switching step.
12. Turn on the washing port and flush the device for 20 sec in order to remove non-trapped contaminating cells.
13. Inject the solution containing the first molecule of interest (0.2 mg/ml of 3,000 Da neutral and anionic dextran molecules or 1.5 mg/ml of 70,000 Da neutral dextran molecule) into the device.
14. Apply five short pulses (Δt= 30 msec with 2 sec intervals) promptly after injection of the molecular solution and monitor the magnitude and duration of the applied electrical pulses in real-time using an oscilloscope.
15. Repeat step 3.10 as many times as the number of additional molecules to be delivered. For each molecular delivery, incubate cells for 100 s in the molecular solution then flush the device with the washing solution for 100 s to remove excess molecules.
16. Release the cells in a 96-well plate for downstream analysis by lowering the operating pressure below 5 psi. NOTE: Approximately 100 µl of solution with 100 cells is collected from each release.
17. Run the experimental steps 3.9 through 3.16 three times to collect enough cells for flow cytometry.
18. Centrifuge the 96-well plate containing processed cells for 5 min at 228 × g.
19. Remove the supernatant that contains excess fluorescent molecules.
20. Resuspend cells in DPBS for flow cytometry analysis.
21. Load cells in the flow cytometer for molecular uptake efficiency analysis.

Representative Results

The developed parallel microfluidic electroporator delivered macromolecules with varied sizes and electrical charges into living metastatic breast cancer cells. Successful molecular delivery was qualitatively determined by monitoring changes in fluorescent intensity of electroporated orbiting cells *in situ* and confirmed by quantitative measurements via flow cytometry analysis. **Figure 4A** shows that 90% of treated cells uptake the 70,000 Da neutral dextran. For the statistical analysis, an intensity threshold for each fluorophore was established such that the majority (>99%) of unprocessed living cells is counted below the threshold (see Figure 4 (**c**)). The efficiency is defined as the ratio of the number of cells successfully taking up the molecules of interest to the total number of processed cells. **Figure 4B** illustrates that the efficiency does not substantially vary depending on molecular weight or electrical charges (P >0.1). All tested dextran molecules were delivered into the cytosol with efficiency greater than 70%. In addition, **Figure 4D** exhibits that sequential molecular delivery was successfully performed with a dual molecule delivery efficiency of 56% using the anionic and neutral dextrans with identical molecular weight (MW = 3,000 Da). The current system can process cells with 10-fold higher throughput and multi-molecule delivery efficiency than the previously reported system[18] and this improvement does not affect single-molecule delivery (82% and 70% for anionic and neutral dextran, respectively).

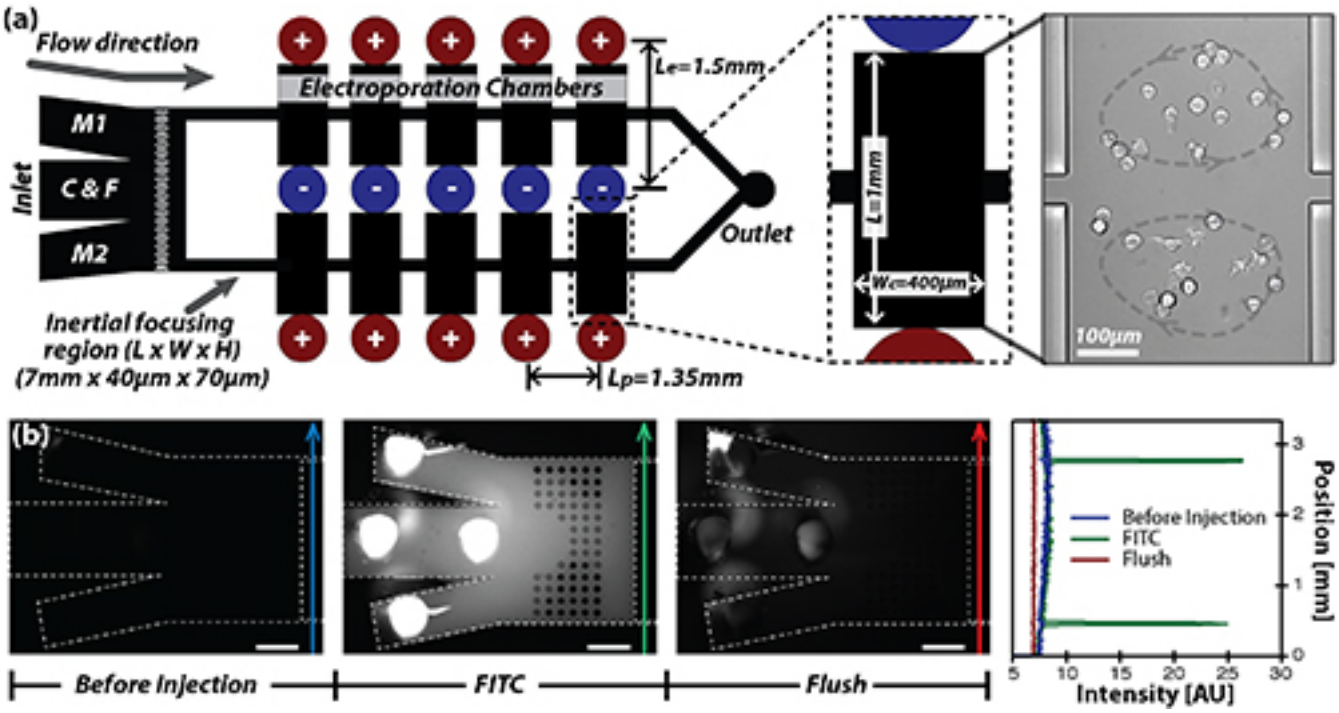

Figure 1. (A) A schematic of the microfluidic electroporation system, consisting of inlets for cells (denoted as C), molecules (denoted as M1 and M2) and a flush solution (denoted as F), two straight channels where inertial focusing occurs, 10 electroporation chambers with electrodes and an outlet. **(B)** Solution exchange demonstration at the inlet using a 1µM FITC solution and a flush solution (DPBS) indicates that the active solution can be uniformly injected to all arrays of chambers downstream. Image contrast is enhanced by adjusting look-up table (LUT). Scale bars are 250 µm. Please click here to view a larger version of this figure.

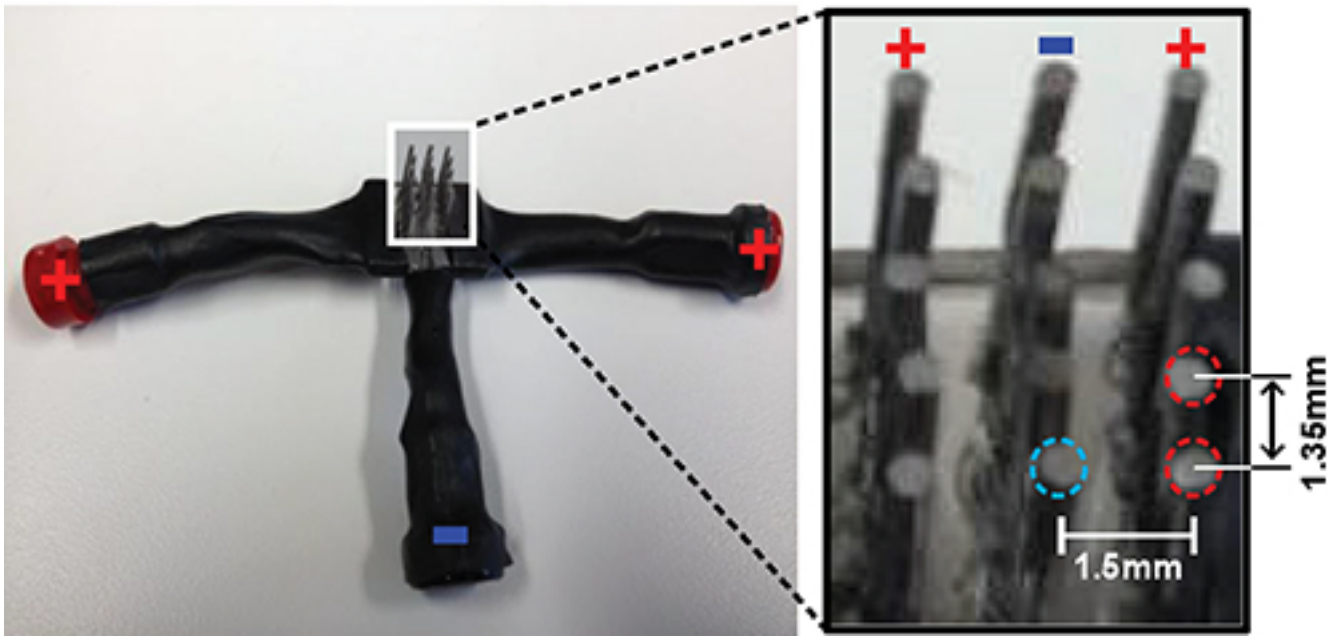

Figure 2. A photograph of the 15-pin electrode utilized for short-pulse high voltage application, consisting of 10 positive (+) and five negative electrodes (-). Each positive electrode is spaced 2 mm apart from a negative electrode, and each electrode of the same polarity is spaced 1.35 mm apart. Please click here to view a larger version of this figure.

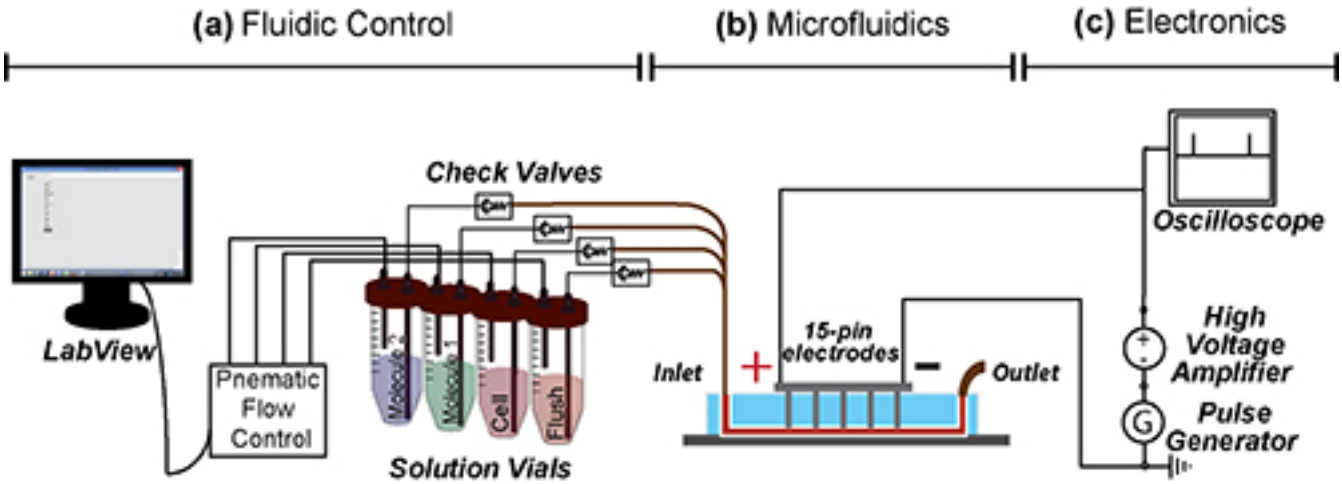

Figure 3. Schematic of the experimental apparatus, consisting of (A) the fluid control unit, (B) the microfluidic electroporator, and (C) the electrical equipment. (A) Vials containing solutions with molecules, cells and clean buffer are individually pressurized on demand using the LabView controlled pneumatic flow system. The solution from the pressurized vial is injected into the microfluidic electroporator through PEEK tubing with a check valve installed. **(B)** and **(C)** The electric signals are sent to 15-pin electrodes in contact with the flowing solution in the microfluidic system during the electroporation step. The electric pulses with the programmed duration are generated using the pulse generator and the magnitude of the electric pulse is amplified to 100 V by the high voltage amplifier. All applied electrical parameters are monitored in real time using an oscilloscope. Please click here to view a larger version of this figure.

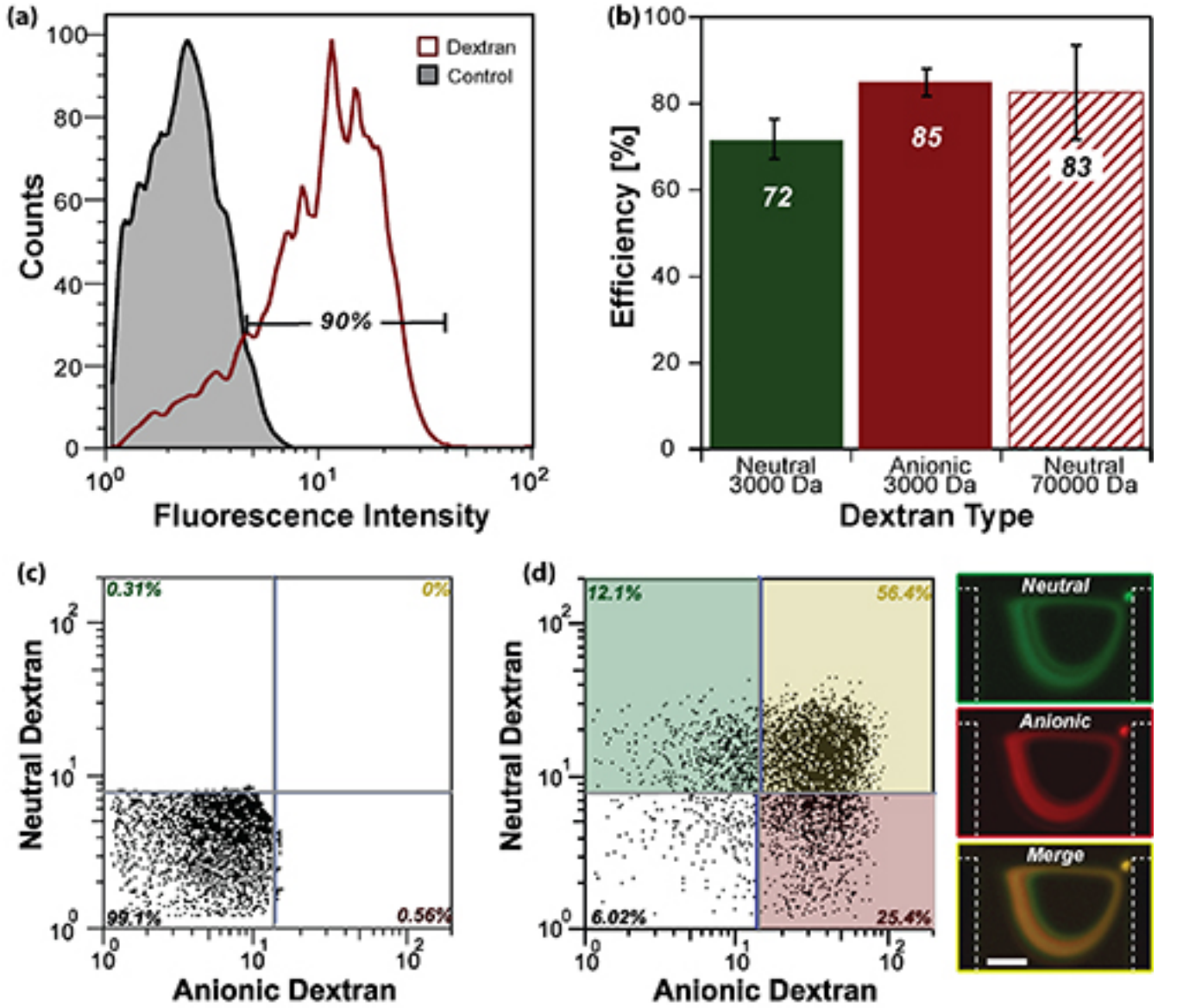

Figure 4. Representative flow cytometry data. (A) Fluorescent signals of MDA-MB-231 cells, which successfully took up the 70,000 Da anionic dextran molecule, compared to that of the control counterpart. **(B)** The efficiencies for each transferred dextran molecule do not exhibit significant molecular dependent variation ($p > 0.1$). **(C)** Representative flow cytometry profiles for cells, which were not treated with electroporation (control). The fluorescent threshold indicating successful molecular delivery is set from the data such that the signals from control samples are found below the threshold. **(D)** Representative flow cytometry data for sequentially electroporated cells. Green, red and yellow boxes in the flow cytometry plot and fluorescent streak images on the right-side represent fluorescent signals from cells uptaking 3,000 Da neutral dextran-only, anionic dextran-only and both dextran molecules, respectively. Scale bar is 100 m. Please click here to view a larger version of this figure.

Discussion

With the new parallelized electroporation platform, 10-fold enhancement in throughput and efficiency of multi-molecule delivery was achieved in addition to all the merits that the previously developed single-chamber system provides.[18] Previously available merits include (i) pre-purification of target cells with uniform size distribution for viability enhancement, (ii) precise and individual molecular dosage control, and (iii) low operational electrical current. Fluorescently labeled dextrans were chosen as molecules of interest because they are readily available in a wide range of molecular weights, conjugated fluorophore types, and electrical charges. These macro-molecules are good candidates for such a study since they are inherently membrane impermeable for living cells and do not exhibit cytotoxicity.[24] Optimum concentration of fluorescent dextran, incubation time, and electrical parameters were identified for the current system prior to the electroporation experiments. The optimization process was rather simple and efficient due to the platform's ability to monitor the molecular uptake process in real-time. Visualization of this process is very beneficial if a molecule or cell type with little-to-no knowledge of electroporation parameters is being tested. The incubation time

for all molecules tested was set to be 100 s by which cells trapped in all 10 chambers exhibit detectable fluorescent intensity signals in real time, indicating the completion of successful molecular delivery. Note that this is not the minimum incubation duration required for molecular delivery.

There has been a long-standing debate regarding the molecular delivery process using electroporation, whether it is solely mediated by diffusion[4,19,25] or by electrophoresis.[26] Identification of the dominant mechanism of molecular delivery involves a series of laborious individual tests, comparing the outcomes depending on molecular sizes, electrical charges and electroporation parameters. To the best of the authors' knowledge, these laborious optimization processes were not reported with conventional electroporation systems.[4,26-28] The developed system's simple parameter optimization capability allowed for identification of the dominant molecular delivery mechanism, by examining variations in the electroporation efficiency depending on molecular and electric parameters. Results showed that the efficiency of anionic 3,000 Da dextran was not significantly different than that of its neutral counterpart (83 and 75%, respectively), suggesting that the molecular uptake observed was possibly mediated by diffusion. Unlike other electroporation systems, processed cells were continuously agitated throughout the electroporation process in this system. Gradual increase in fluorescent signals of orbiting cells was observed, suggesting that diffusion would be the dominant delivery mechanism. High efficiency molecular uptake (90%) of neutral 70,000 Da dextran molecules further implies that even at high molecular weights the delivery process occurs as a result of diffusion. Lastly, successful sequential delivery of 3,000 Da anionic and neutral dextran molecules solidifies the claim that molecular delivery occurs despite the molecules charge. This result also suggests that membrane resealing is not completed within 3 min of electroporation (100 sec per molecular delivery).

The presented molecular delivery platform can sequentially deliver wide ranges of molecular sizes regardless of their electrical charges. Timely fine-tuning and modification of individual parameters can be achieved with little effort aided by the real-time process monitoring capability. The system's size-based cell purification process eliminates the need for laborious sample preparation and time-consuming centrifugation pre- and post-electroporation steps. Furthermore, the system's low operational current substantially reduces cell mortality.

Disclosures

The authors have nothing to disclose.

Acknowledgements

This work is supported by the Rowland Junior Fellow program. The authors would like to express gratitude to the scientists and staff at the Rowland Institute at Harvard: Chris Stokes for his help in the development of the custom-built, computer-assisted pressure control setup, Diane Schaak, Ph.D. for her input for biological sample handling, Winfield Hill for developing the electrical setup, Alavaro Sanchez, Ph.D. for granting access to the flow cytometer, Scott Bevis, Kenny Spencer and Don Rogers for machining mechanical plumbing components required for the pressure setup. Microfluidic masters were fabricated at the Center for Nanoscale Systems (CNS) at Harvard University.

References

1. Nakamura, H., & Funahashi, J. Electroporation: Past, present and future. *Dev. Growth Diff.* **55**, 15-19, doi:10.1111/dgd.12012 (2013).
2. Geng, T., & Lu, C. Microfluidic electroporation for cellular analysis and delivery. *Lab Chip.* **13**, 3803-3821, doi:10.1039/c3lc50566a (2013).
3. Shahini, M., van Wijngaarden, F., & Yeow, J. T. W. Fabrication of electro-microfluidic channel for single cell electroporation. *Biomedical Microdevices.* **15**, 759-766, doi:10.1007/s10544-013-9761-0 (2013).
4. Neumann, E., Toensing, K., Kakorin, S., Budde, P., & Frey, J. Mechanism of electroporative dye uptake by mouse B cells. *Biophysical Journal.* **74**, 98-108 (1998).
5. Jaroszeski, M. J. *et al.* Toxicity of anticancer agents mediated by electroporation *in vitro*. *Anti-Cancer Drugs.* **11**, 201-208, doi:10.1097/00001813-200003000-00008 (2000).
6. Buntru, M., Gartner, S., Staib, L., Kreuzaler, F., & Schlaich, N. Delivery of multiple transgenes to plant cells by an improved version of MultiRound Gateway technology. *Transgenic Res.* **22**, 153-167, doi:10.1007/s11248-012-9640-0 (2013).
7. Mir, L. M. *et al.* High-efficiency gene transfer into skeletal muscle mediated by electric pulses. *Proc. Natl. Acad. Sci. U. S. A.* **96**, 4262-4267, doi:10.1073/pnas.96.8.4262 (1999).
8. Heller, R. *et al.* Intradermal delivery of interleukin-12 plasmid DNA by *in vivo* electroporation. *DNA Cell Biol.* **20**, 381-381 (2001).
9. Boukany, P. E. *et al.* Nanochannel electroporation delivers precise amounts of biomolecules into living cells. *Nat. Nanotechnol.* **6**, 747-754, doi:10.1038/nnano.2011.164 (2011).
10. Wang, J. *et al.* Synergistic Effects of Nanosecond Pulsed Electric Fields Combined with Low Concentration of Gemcitabine on Human Oral Squamous Cell Carcinoma *In Vitro*. *PLoS One.* **7**, doi:e4321310.1371/journal.pone.0043213 (2012).
11. Kim, M. J., Kim, T., & Cho, Y. H. Cell electroporation chip using multiple electric field zones in a single channel. *Appl. Phys. Lett.* **101**, doi:22370510.1063/1.4769037 (2012).
12. Wang, S. N., & Lee, L. J. Micro-/nanofluidics based cell electroporation. *Biomicrofluidics.* **7**, doi:01130110.1063/1.4774071 (2013).
13. Sharei, A. *et al.* A vector-free microfluidic platform for intracellular delivery. *Proc. Natl. Acad. Sci. U. S. A.* **110**, 2082-2087, doi:10.1073/pnas.1218705110 (2013).
14. Kim, J. B. *et al.* Direct reprogramming of human neural stem cells by OCT4. *Nature.* **461**, 649-U693, doi:10.1038/nature08436 (2009).
15. Ozbas-Turan, S., Aral, C., Kabasakal, L., Keyer-Uysal, M., & Akbuga, J. Co-encapsulation of two plasmids in chitosan microspheres as a non-viral gene delivery vehicle. *J. Pharm. Pharm. Sci.* **6**, 27-32 (2003).
16. Okita, K., Ichisaka, T., & Yamanaka, S. Generation of germline-competent induced pluripotent stem cells. *Nature.* **448**, 313-U311, doi:10.1038/nature05934 (2007).
17. Hur, S. C., Mach, A. J., & Di Carlo, D. High-throughput size-based rare cell enrichment using microscale vortices. *Biomicrofluidics.* **5**, doi:02220610.1063/1.3576780 (2011).
18. Yun, H. Y., & Hur, S. C. Sequential multi-molecule delivery using vortex-assisted electroporation. *Lab Chip.* **13**, 2764-2772, doi:10.1039/c3lc50196e (2013).

19. Gehl, J. Electroporation: theory and methods, perspectives for drug delivery, gene therapy and research. *Acta Physiol. Scand.* **177**, 437-447, doi:10.1046/j.1365-201X.2003.01093.x (2003).
20. Wang, J., Zhan, Y. H., Ugaz, V. M., & Lu, C. Vortex-assisted DNA delivery. *Lab Chip.* **10**, 2057-2061, doi:10.1039/c004472e (2010).
21. Jia, F. J. *et al.* A nonviral minicircle vector for deriving human iPS cells. *Nature Methods.* **7**, 197-U146, doi:10.1038/nmeth.1426 (2010).
22. Dunbar, C. E. Gene transfer to hematopoietic stem cells: Implications for gene therapy of human disease. *Annual Review of Medicine.* **47**, 11-20 (1996).
23. Xia, Y. N., & Whitesides, G. M. Soft lithography. *Angew. Chem.-Int. Edit.* **37**, 551-575 (1998).
24. Graziadei, L., Burfeind, P., & Barsagi, D. Introduction of Unlabeled Proteins into Living Cells by Electroporation and Isolation of Viable Protein-Loaded Cells Using Dextran Fluorescein Isothiocyanate as a Marker for Protein-Uptake. *Anal. Biochem.* **194**, 198-203, doi:10.1016/0003-2697(91)90168-s (1991).
25. Dimitrov, D. S., & Sowers, A. E. Membrane Electroporation-Fast Molecular-Exchange by Electroosmosis. *Biochimica Et Biophysica Acta.* **1022**, 381-392, doi:10.1016/0005-2736(90)90289-z (1990).
26. Sukharev, S. I., Klenchin, V. A., Serov, S. M., Chernomordik, L. V., & Chizmadzhev Yu, A. Electroporation and electrophoretic DNA transfer into cells. The effect of DNA interaction with electropores. *Biophysical Journal.* **63**, 1320-1327, doi:http://dx.doi.org/10.1016/S0006-3495(92)81709-5 (1992).
27. Glogauer, M., & McCulloch, C. A. G. Introduction of large molecules into viable fibroblasts by electroporation: Optimization of loading and identification of labeled cellular compartments. *Experimental Cell Research.* **200**, 227-234, doi:http://dx.doi.org/10.1016/0014-4827(92)90168-8(1992).
28. Verspohl, E. J., KaiserlingBuddemeier, I., & Wienecke, A. Introducing specific antibodies into electropermeabilized cells is a valuable tool for eliminating specific cell functions. *Cell Biochemistry and Function.* **15**, 127-134, doi:10.1002/(sici)1099-0844(19970601)15:2<127::aid-cbf732>3.0.co;2-e (1997).

